Int j simul model 23 (2024) 3, 519-530
Original scientific paper

FINITE ELEMENT STUDY ON THE EFFECT OF FIBRILLAR MORPHOLOGY ON CORNEAL BIOMECHANICS

Han, S. F.[*,#]; Miao, Y. R.[*]; Pei, Y. J.[**] & Yang, Y.[***]
[*] School of Energy Power and Mechanical Engineering, North China Electric Power University, Beijing 102206, China
[**] Department of Ophthalmology, Shanxi Eye Hospital Affiliated to Shanxi Medical University, Taiyuan 030002, China
[***] School of Mechanical Engineering and Automation, Beihang University, Beijing 100191, China
E-Mail: shaofenghan@foxmail.com, m3047592353@163.com, 18535463503@163.com, yang_mech@126.com ([#] Corresponding author)

Abstract
Understanding the relationship between fibril morphology and corneal biomechanics is crucial for predicting the ocular response to physiological and surgical loads. In this study, we developed a finite element model of the corneal strip to investigate the effect of fibril crimp parameters, area fraction and orientation on the nonlinear stress-strain behaviour. The fibrils were modelled as Ogden materials with a Gaussian distributed crimp degree, while the matrix was set linear elastic. Uniaxial tension simulations were performed to analyse the evolution of fibril deformation and stress with the applied load. The result showed good agreement with the experimental data reported in the literature and captured the three stages of corneal response. Increasing the fibril area fraction, and decreasing the crimp degree and angular deviation from the loading axis resulted in higher corneal stiffness. Interestingly, the stress-strain behaviour was insensitive to changes in crimp amplitude and period at a constant crimp degree. These findings provide novel insights into the corneal structure-function relationships and highlight the potential of multi-scale computational models for predicting ocular biomechanics.
(Received in April 2024, accepted in July 2024. This paper was with the authors 6 weeks for 2 revisions.)

Key Words: Fibril Morphology, Finite Element Model, Corneal Strip, Stress-Strain Behaviour, Uniaxial Tension

1. INTRODUCTION

The essential function of the human cornea is to protect outer objects from entering into the eye and as a main refractive element for focusing light on the retina [1]. The cornea comprises five layers: the epithelium, Bowman's layer, the stroma, Descemet's membrane, and the endothelium. The stroma constitutes approximately 90 % of the total thickness [2]. Furthermore, the nonlinear biomechanics of the stroma is primarily determined by the architecture of the underlying collagen [3]. Understanding the connection between fibril arrangement and the mechanical characteristics of the cornea is crucial for elucidating corneal pathologies related to abnormal microstructure. Currently, multi-scale studies of the cornea mainly rely on experiments and the construction of constitutive equations [4, 5], lacking quantitative analysis of the effect of fibril crimp parameters on corneal biomechanics. Therefore, it is necessary to explore the use of finite element methods to study the influence of fibrillar morphology on the cornea.

Corneal fibrils have been studied intensively using various imaging techniques, such as optical and non-optical methods. Optical methods include fluorescence microscopy [6], polarized light [7], confocal microscopy [8], and nonlinear optical imaging [1]. Non-optical methods include scanning electron microscopy (SEM) [9] and transmission electron microscopy (TEM) [10]. Optical methods are commonly used to analyse the distribution of fibrils. While non-optical methods can image the individual collagen fibril to obtain morphological parameters. Additionally, X-ray diffraction studies have revealed that the preferred orientations of collagen fibrils are in the nasal-temporal and superior-inferior directions [11].

Fibril crimp morphology plays a crucial role in nonlinear corneal behaviour. Comninou and Yannas [12] modelled fibrils as long, sinusoidal beams in connective tissues, and established a constitutive equation for uniaxial tension by considering a single fibril and bundles of fibrils embedded in a matrix. Grytz and Meschke [13] proposed a constitutive model of crimped collagen fibril networks to investigate the interaction between fibril architecture and loading conditions in a human eye model. In this model, a single collagen fibril was approximately predicted to be a helical spring, reflecting the nonlinear mechanical properties of fibrils. Liu et al. [10] constructed a model assuming that the morphology of crimp fibrils followed a Gaussian distribution and observed the crimping degree of fibrils under different tensile loads using TEM. Jan et al. [14] quantified the collagen crimp morphology across the corneoscleral shell and obtained the median crimp parameters for the whole eye globe.

Simulations are viewed as important means for overcoming the constraints imposed by limited data points. The corneal model taking microstructure of the stroma into account was earliest introduced by Pinsky and Datye [15] to simulate radial keratotomy (RK). Subsequently, based on the orientation and distribution of fibrils, a series of constitutive models were introduced for finite element modelling to analyse standard ophthalmic procedures, such as photorefractive keratectomy (PRK) and limbal relaxing incisions (LRI) [16, 17]. Giraudet et al. [18] built a multi-scale model of the cornea and constructed its constitutive equation based on an energy function to simulate the mechanical response of healthy and pathological corneas under intraocular pressure. Gomez et al. [19] proposed a corneal multizone-based model to study the influence of boundary conditions on corneal deformation. Additionally, Petsche and Pinsky [20] proposed a three-dimensional lamella model with a depth-dependent inclination distribution.

Previous simulation studies have mainly considered the cornea as a homogeneous material or constructed corresponding constitutive models, discounting variations in its intrinsic structure. In this study, to investigate the biomechanical roles of multi-scale computational modelling in corneal microstructure, we developed a corneal strip model with crimped collagen fibrils to analyse the biomechanical behaviour of the cornea. The fibrils are randomly distributed in the cornea, and the length of fibrils follows a Gaussian distribution. Through uniaxial tension, the load-elongation relationship correlates well with the experimental data. Moreover, the nonlinear characteristics of the area fraction, crimp degree and direction of the fibrils were also analysed. Our simulation method provides a more realistic model necessary to build ocular biomechanics and remodelling.

2. MATERIAL AND METHODS

2.1 Single fibril parameters

Since the fibril crimps are wavy, in order to clearly describe the crimp characteristics of fibrils, each crimp fibril was defined and quantified using three critical parameters: period, amplitude, and crimp degree, as illustrated in Fig. 1. The expression of a single fibril can be described as:

$$y = Asin(2\pi nx) \tag{1}$$

where, *A* represents the amplitude, and *n* denotes the total number of periods of a single fibril. When the amplitude and length of the corneal strip are set as constants, the crimp degree is determined by the period. A larger period corresponds to a smaller crimp degree, while a smaller period results in a larger crimp degree.

The arc length of a single fibril can be expressed as:

$$s = ns_{one} \tag{2}$$

where, s_{one} is the arc length of the fibril in one period. Setting the length of the corneal strip to 1, s_{one} can be expressed as:

$$s_{one} = 4\int_0^{\frac{1}{4n}} \sqrt{1+(y')^2}\,dx = 4\int_0^{\frac{1}{4n}} \sqrt{1+(2A\pi n\cos 2\pi nx)^2}\,dx = \frac{2}{\pi n}\int_0^{\frac{\pi}{2}} \sqrt{1+(2A\pi n\cos x_1)^2}\,dx_1 \tag{3}$$

Expanding Eq. (3) into a Taylor series, we can obtain:

$$s_{one} = \frac{2}{\pi n}\int_0^{\frac{\pi}{2}} \left(1+\frac{1}{2}(2A\pi n)^2\cos^2 x_1 - \frac{1}{2!\,2^2}(2A\pi n)^4\cos^4 x_1 + \frac{3}{3!\,2^3}(2A\pi n)^6\cos^6 x_1 \cdots\right)dx_1 \tag{4}$$

From the integral formula $\int_0^{\frac{\pi}{2}} cos^{2n}\,dx = \frac{\pi(2n)!}{2^{n+1}n!n!}$, s_{one} can be described as:

$$s_{one} = \frac{2}{\pi n}\left(\frac{\pi}{2}+\frac{1}{2}(2A\pi n)^2\frac{\pi 2!}{2^2} - \frac{1}{2!\,2^2}(2A\pi n)^4\frac{\pi 4!}{2^3 2!\,2!} + \frac{3}{3!\,2^3}(2A\pi n)^6\frac{\pi 6!}{2^7 3!\,3!}\cdots\right) \tag{5}$$

Therefore, s can be written as:

$$s = 1 + 2(A\pi n)^2 - 3(A\pi n)^4 + \frac{5}{4}(A\pi n)^6 \cdots \tag{6}$$

Eq. (6) demonstrates that the arc length of a single fibril is determined by the amplitude A and the number of periods n. When the length of the corneal strip and the amplitude of the fibrils are fixed, the crimp degree is determined by the period. As the period approaches infinite, the crimp degree is close to 1, and as the period becomes infinitesimal, the crimp degree tends towards infinity.

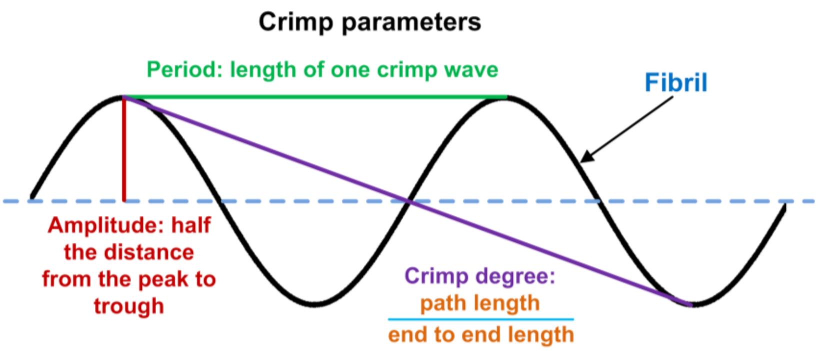

Figure 1: Definitions of the crimp parameters, including period, amplitude, and crimp degree.

2.2 Corneal strip model

Tensile or compression tests are conventional and universally used methods to measure the material properties, reflecting the stress-strain relationship of the material [21, 22]. Strip specimens are typically cut into 2-3 mm width, and with a specimen length of 12 mm length, and with a clamp distance of 4-6 mm [10, 21]. The diameter of corneal fibrils is approximately 30 nm [23], and the area fraction of fibrils occupies less than 50 % of the total corneal cross section [24]. Considering the vast difference between cornea and fibrils sizes, the number of meshes is at least tens of millions, so it is almost impossible to simulate with the default physical size. After testing, it was found that when the length, width, and height of the corneal strip were set to 1.5 mm, 0.5 mm and 0.125 mm, respectively, with the diameter of fibrils chosen to be 0.009 mm, and the area fraction of fibrils set to 5 % [25], the corneal strip can carry out finite element calculation and reflect the changes of fibrils well. The parameters are listed in Table I.

To determine the impact of different parameters, and fibril morphology on corneal biomechanics, a base model, was constructed. As per the previous report on median crimp value measurements, the amplitude was set to a constant 0.0063 mm (10 times larger) [26]. The generated crimp degree (or tortuosity) complied with a Gaussian distribution [10]; the expectation μ was set at 1.007 [26], and the standard deviation σ was set at 0.0781 [10]. The geometric model of the corneal strip is shown in Fig. 2. The strip was composed of fibrils and an interfibrillar matrix (substances other than fibrils). During the stretching process, the corneal strip was fixed at one end and stretched at the other end, and with the maximum strain rate set to 0.36.

Table I: Parameters of the corneal strip used in the simulation.

Name	**Parameters**	**Base values**
Corneal strip	Length (mm)	1.5
	Width (mm)	0.5
	Height (mm)	0.125
Fibrils	Area fraction (%)	5
	Diameter (mm)	0.009
	Amplitude (mm)	0.0063
	Expectation μ	1.007
	Standard deviation σ	0.0781

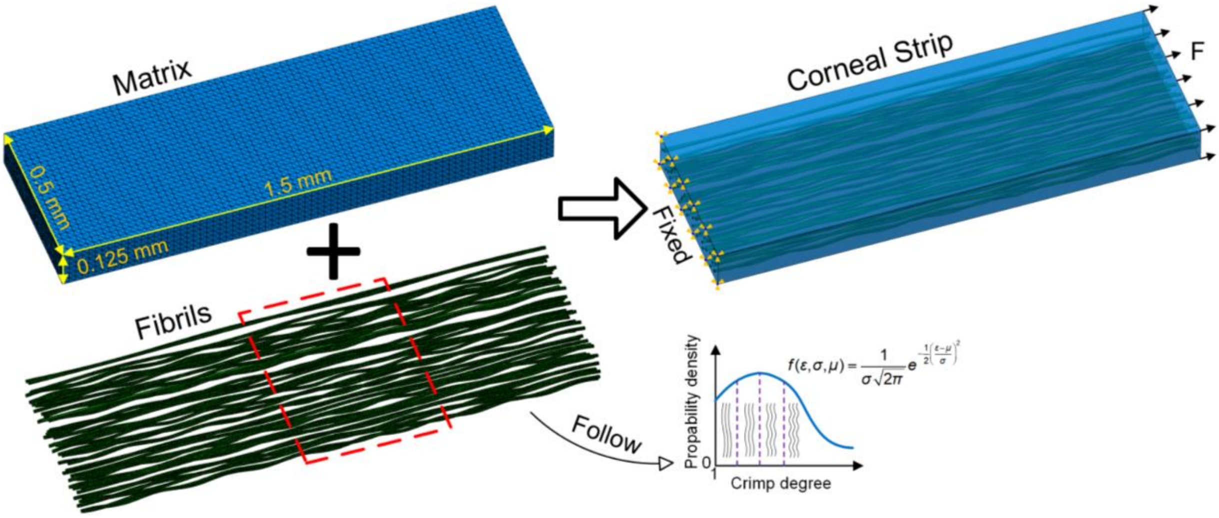

Figure 2: Construction of the corneal strip model.

In the elastic stage of small deformation, it is considered that the fibrils have not been stretched, and the matrix bears the main force. In this study, the matrix is considered to be elastic, with a Poisson's ratio v of 0.48 and Young's modulus E of 0.2 MPa [27]. To simulate the fibrils mechanical behaviour, the first-order, hyperelastic Ogden material model was used:

$$W = \frac{2\eta}{\alpha^2}(\bar{\lambda}_1^\alpha + \bar{\lambda}_2^\alpha + \bar{\lambda}_3^\alpha - 3) + \frac{1}{D}(J-1)^2 \tag{7}$$

where, $\bar{\lambda}_k$ ($k = 1, 2, 3$) represents the deviatoric principal stretch, which is $J^{-1/3}\lambda_k$ ($k = 1, 2, 3$). λ_k represents the principal stretch, D is the inverse of the bulk modulus, J represents Jacobian determinant of the deformation gradient tensor F, and α and η are the material constants. The values of α and η were obtained as 29.5 and 1, respectively, according to the data from an inverse modelling procedure to choose suitable parameters, that fit well with previously reported experimental data [27].

The model of the corneal strip was constructed using a Python script. Fibrils were meshed with the elements of C3D4H (4-node linear tetrahedron and hybrid formulation), and the matrix was set to C3D4 (ABAQUS 6.14). The contact between fibrils and matrix was set as a tie constraint, which constrains the relative deformation and motion between adjacent surfaces of fibrils and matrix. An encastre constraint was applied to one end of the corneal strip, and displacement was set at the other end. The mesh of the fibrils was refined to ensure the accuracy of the numerical simulation, and the number of fibrils and matrix elements were 425162 and 2658282, respectively.

2.3 Simulation conditions

The area fraction and morphology of collagen fibrils are various with individual differences [28]. To explore the effect of this parameter, fibril volume ratios of 2 %, 5 %, 7.5 %, and 10 % were discussed in this study. The crimping morphology of fibrils is determined by specific parameters, and the crimp degree is a crucial parameter to influence the corneal biomechanical behaviour. According to previously reported established values, the crimp degree varies from 1.005 to 1.063 [10, 26]. In this study, we chose 1.007, 1.034, and 1.063 as the average values of the simulated crimp degree.

Additionally, the orientation of the fibrils is also essential, potentially affecting the corneal curvature. The fibrils are preferentially oriented in two directions: horizontal (nasal-temporal) and vertical (inferior-superior) [29]. The selection of corneal strip direction might lead to angle differences between the fibril direction and the length direction of the corneal strip. Angles of 10°, 15°, and 45° were simulated to compare the nonlinear behaviour.

In this study, we have discussed the corneal strip stretching stage without emphasizing the breaking of fibrils.

3. RESULTS

The load-elongation relationship obtained in the numerical simulation is depicted as a solid black line in Fig. 3. The cornea was initially in low-stiffness region, and with the increase of the elongation, it entered into the region of higher stiffness. The curve can be divided into three sections: OA, AB, and BC. In the OA segment, elongation increased rapidly while the change in load was relatively lower and maintained at a low value, and the stiffness is 0.08 N/mm. The AB segment showed a nonlinear exponential growth relationship between load and elongation. In the last BC segment, the load was nearly linear to the elongation with a stiffness of 3.62 N/mm under large deformation. In this case, the expected value of the frequency was 26.6 Hz.

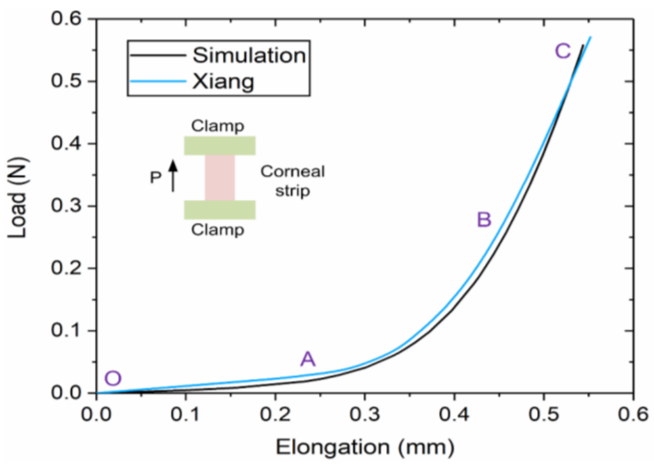

Figure 3: Uniaxial tensile load-elongation curves from the current simulation and the experimental result from Xiang et al. [27].

According to theoretical calculation, when the fibril is straightened, it needs to be stretched 0.27 mm, which is basically corresponding to the simulation. Meanwhile, the results obtained by a finite element simulation model fits well with the corneal strip stretching experimental data that Xiang et al. [27] has obtained ($R^2 = 0.997$), with stiffness values of 0.11 N/mm and 3.13 N/mm under small and large deformation, respectively. The analysis validates that the corneal strip model constructed in this work can predict and compare the mechanical behaviours of the cornea under various conditions.

The deformation and stress of fibrils with the increase of elongation δ are illustrated in Fig. 4. In the initial stretching stage (Fig. 4 A-C), corresponding to the OA segment of the curve, most fibrils were in the state of relaxation, and the tensile stress was small. With the increase of elongation (Fig. 4 D-F), the fibrils gradually straightened and began to experience force, and displaying nonlinear behaviour (AB segment). When approximately all fibrils were stretched (Fig. 4 G-I), the slope of the stress-strain curve remained constant, reflected in the BC segment of the curve.

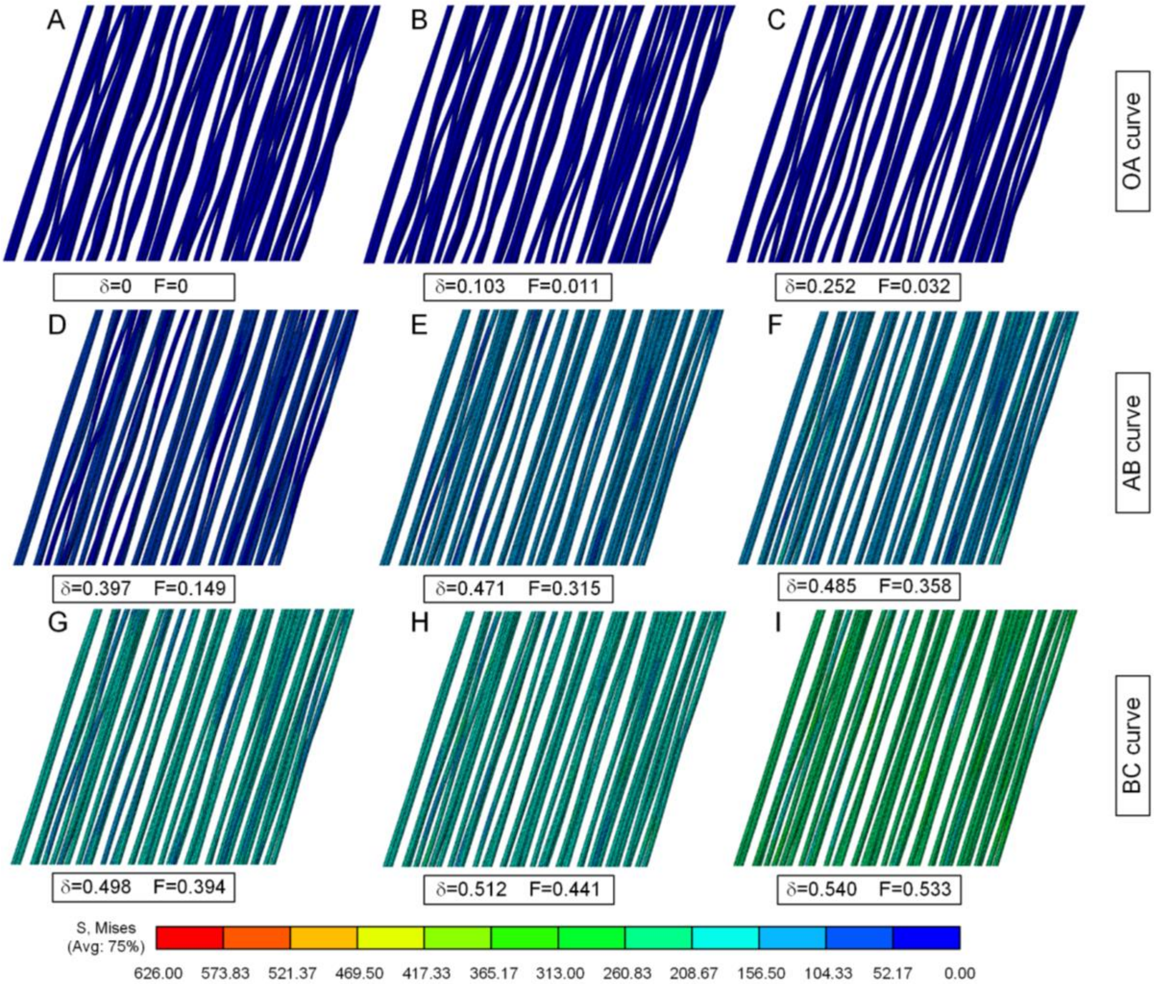

Figure 4: Deformation and stress nephogram of fibrils under different elongations in the red dotted frame of Fig. 2.

Fig. 5 demonstrates the mechanical behaviours curves of the corneal strip with four different area fractions of fibrils, 2 %, 5 %, 7.5 %, and 10 %. The crimp degree kept constant at 1.007. At 2 % area fraction, the nonlinear behaviour was not prominent. However, as the fibril area fraction increased, the corneal behaviour became steeper, a typical characteristic of hyperelasticity. At a constant strain of 0.36, we also noticed a steady increment of stress level from 4.70 MPa at 2 % fibril area fraction to 17.63 MPa (375 %) at 10 % fibril area fraction.

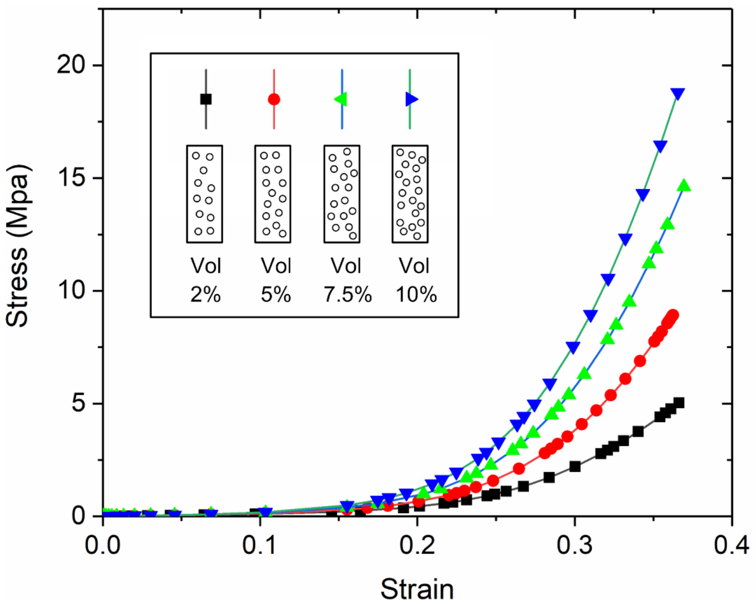

Figure 5: Uniaxial tensile stress-strain curves at the fibril volumes of 2 %, 5 %, 7.5 %, and 10 %; the crimp degree keeps constant at 1.007.

For a single fibril, when the amplitude is set to a fixed value, the crimp degree ε is determined by the angular frequency ω. In a corneal strip, the fibrils follow a Gaussian distribution. Fig. 6 discusses the stress-strain relationships under different crimp degrees: 1.007, 1.034 and 1.063. An inverse relationship between the crimp degree and stiffness of the curve was observed. At a constant strain of 0.36, as the crimp degree increased from 1.007 to 1.063, the stress decreased by 22.63 %.

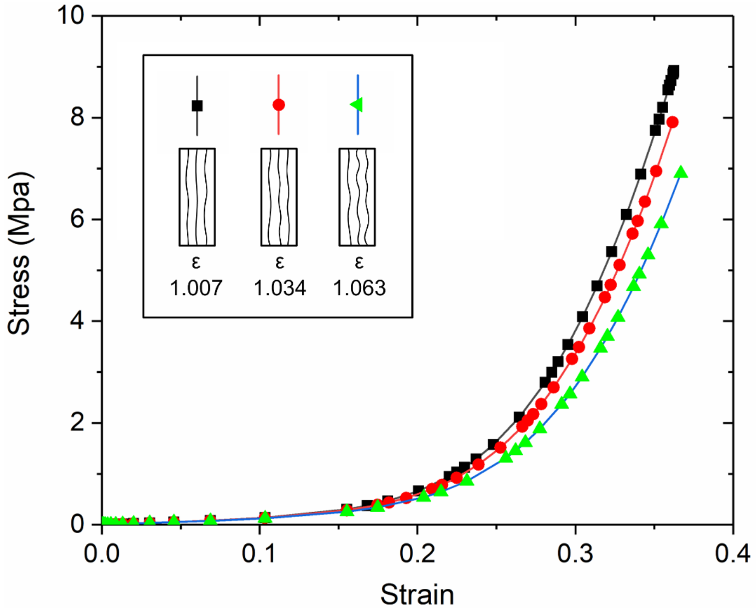

Figure 6: Uniaxial tensile stress-strain curves at the crimp degrees of 1.007, 1.034 and 1.063.

Fig. 7 illustrates the stress-strain relationship at four different angles between directions of fibrils and length of the corneal strip. The angle has a significant impact on the change in stress. In the absence of complete fibrils passing through the corneal strip in the stretch direction, the stress declines significantly. For example, at a strain of 0.36, the stress at 45° is only 0.055 MPa, approximately 1/160 of the stress at 0°.

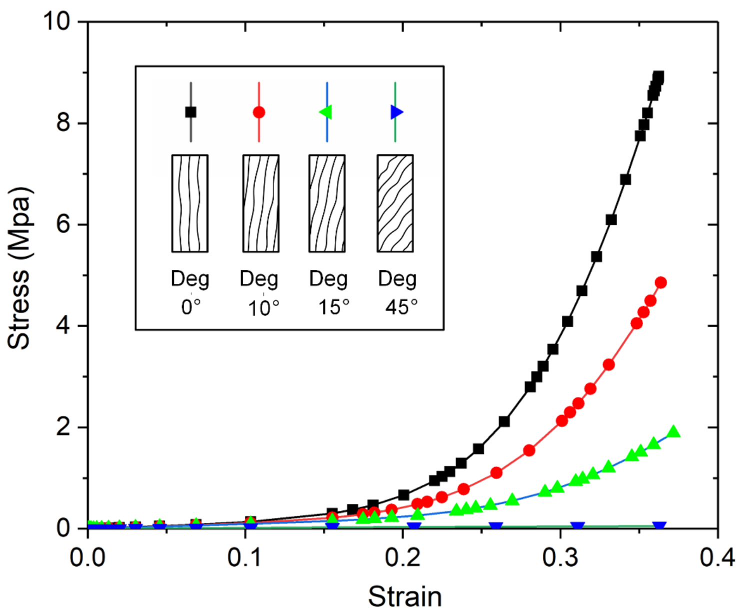

Figure 7: Uniaxial tensile stress-strain curves at the angles of 0°, 10°, 15° and 45° between the fibrils and corneal strip.

The maximum stress at a strain of 0.36 under the same crimp degree but different amplitudes is explained below in Fig. 8. When the crimp degree remained the same, the stress at amplitudes of 0.0035 mm, 0.005 mm, and 0.0063 mm was essentially consistent, with fluctuations not exceeding 10 %. At the crimp degree of 1.007, the stresses were 9.33 MPa, 9.22 MPa, and 8.73 MPa, while at the crimp degree of 1.063, the stresses were 7.12 MPa, 6.67 MPa, and 6.48 MPa.

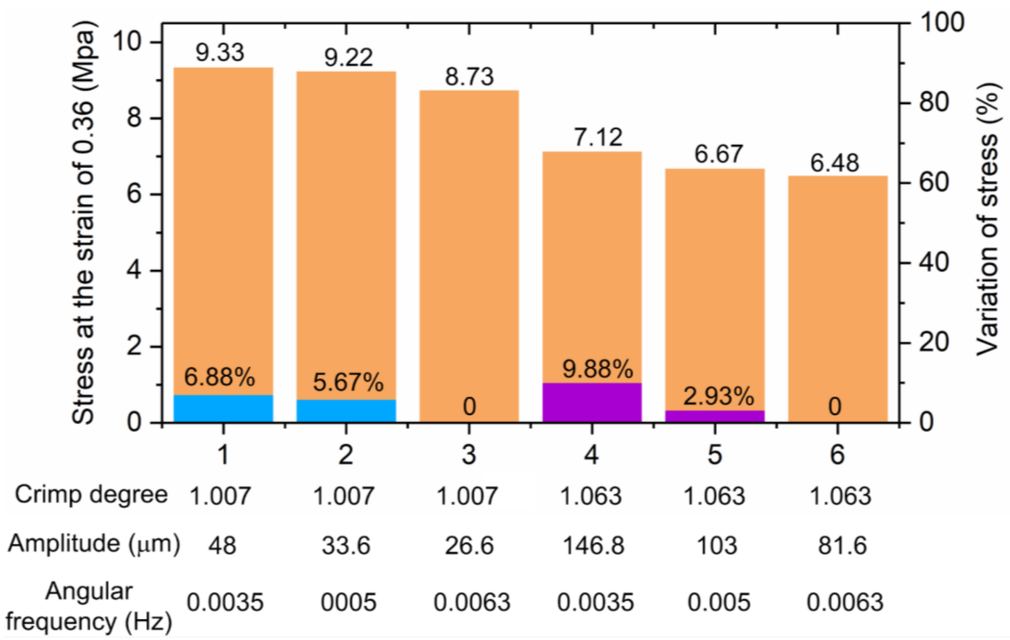

Figure 8: Uniaxial tensile stress-strain curves under different angles of fibrils and corneal strip.

4. DISCUSSION

This study presents a finite element corneal strip model utilized to investigate the relationship between the crimping morphology of collagen fibrils and the non-linear biomechanical behaviour of the cornea. The parallel arrangement of fibrils is crucial for maintaining corneal transparency. This study employed a finite element corneal strip model considering the morphology of crimped fibrils, which keeping the same orientation. The tensile simulations observed in this study are in corroboration with previous reports and are reproducible. The biomechanics of the corneal strip were analysed under the effect of area fraction, crimp degree, and angles of fibrils. Previous studies have considered the cornea either as an isotropic material or as a constitutive model, taking into account the orientation of the fibrils [30]. The model presented in this study provides a novel method for corneal construction that can couple the change in mechanics with changes in geometry. The three different stages during the stretching process can be reflected from fibrils. We observed an increment in fibrillar tension with the change in fibrillar structure, particularly when it was straightened. Furthermore, with the increased number of fibrillar stretches, the tangent modulus of the corneal strip increased significantly.

The strip testing adopted in this study is a standard method to obtain tissue biomechanics and has been extensively used in previous studies [31]. Even though in the strip testing method, the uniaxial loading is different from the loading existed *in vivo* (whole eye globes), and may cause changes in the overall behaviour obtained, it remains an acceptable and viable method in the field. This method is particularly useful in comparative studies, such as comparing different parameters in tissue while observing nonlinear behaviour. Several studies have successfully employed strip testing techniques to investigate the effect of parameters of interest on tissue behaviour [10, 32].

The morphology of fibrils is the primary contributor to the material nonlinear biomechanical behaviour [33]. In this study, we have demonstrated that stress level increases with the increment in the fibrillar area fraction (Fig. 5). As the volume of fibrils increases, the universal stiffness of the corneal strip also increases. This is because the fibrils play a major role in bearing load during stretching. Therefore, stretching unit length requires more force than usual to be loaded. This supports the notion that the fibrils will become increasingly unfolded as the corneal pressure increases above physiological pressure, contributing to the increase in tissue stiffness [34]. As explained in our uniaxial tensile stress-strain curve, with the expectation of an increment in the crimp degree, to reach the same stress value, the strain of fibrils would rise (Fig. 6). We speculate that due to the increase of crimp degree, a greater tensile length is needed to straighten the fibres, or the corneal strip requires more strain to apply the same stress to the fibrils.

The uneven distribution of fibrils contributes to corneal anisotropy [12]. When preparing the corneal strips, there is a possibility of forming different angles between the stretching direction of the corneal strip and fibrillar direction. We observed a significant decline in the stress curve at the angle of 45° (Fig. 7). We postulate that during the stretch simulation, the fibrils were not subjected to stress, and only the matrix experienced tension [34]. Notably, the fibrils consistently remained in a state of relaxation. The primary reason of the decrease of the stiffness is the weakening of the collagen fibrils, consistent with the disorganization of the lamellae observed in Meek et al. [35]. Identifying the area with weaker fibrils could facilitate the implementation of stiffening treatment measures. We propose that the direction of corneal strip selection is a crucial factor that affects the nonlinear relationship.

It is reported that the amplitude and period establish an inverse relationship, especially when they have similar crimp degrees. A fibril with a large amplitude always displays a low period, and a fibril with a small amplitude always displays an extensive period [4]. We investigated this phenomenon in our study by comparing simulations at a strain of 0.36 with the same crimp degree but different amplitude and period (Fig. 8). The observed stress values were similar at the same crimp degree, indicating that the crimp degree is the key parameters in determining whether fibrils straighten under a specific stretching length. Only when the fibrils are straightened can they begin to bear the force. Interestingly, the amplitude and period do not appear to be the determinants of corneal biomechanical properties.

The current corneal strip model has limitations that require further development. A critical challenge is the significant difference in corneal and fibril size. It is difficult to simulate with the default size of fibrils, so obtaining a size of bigger diameter can be considered as fibril bundles. We observed that when the diameter of fibrils is increased by 300 times, the stress-strain curve lies within the range of the experimental data, enabling model simulation. In addition, it is noteworthy that the orientation and diameter of fibrils vary across different regions of the cornea. To simplify the model, the orientation of fibrils was set along the length of the strip specimen and distribution was modelled using a Gaussian model. Also, the diameter was set uniform value. The matrix and fibrils were considered elastic and hyperelastic materials, respectively, and there may also exist material combinations that better represent the mechanical properties of the cornea.

5. CONCLUSION

In this study, we developed a novel finite element model of the corneal strip that incorporates realistic representations of collagen fibril morphology and distribution. The model successfully captured the nonlinear biomechanical behaviour of the cornea under uniaxial tension and revealed the significant influence of fibril crimp parameters, area fraction, and orientation on tissue stiffness and anisotropy. The key contributions of this work are threefold: 1) a mathematical formulation for describing fibril crimp geometry and statistical distribution; 2) a multi-scale computational framework for linking fibril mechanics to tissue-level response; and 3) new insights into the structure-function relationships of the cornea and the potential mechanisms underlying its nonlinear behaviour. In the future, we will explore the effect of fibril microstructure on the biomechanics of a more realistic three-dimensional corneal model.

ACKNOWLEDGEMENT

This study was supported by the National Natural Science Foundation of China (No. 12202144), the Fundamental Research Funds for the Central University (No. 2022MS008) and the National Key R & D Program of China (No. 2017YFB1302702).

REFERENCES

[1] Winkler, M.; Shoa, G.; Xie, Y.; Petsche, S. J.; Pinsky, P. M.; Juhasz, T.; Brown, D. J.; Jester, J. V. (2013). Three-dimensional distribution of transverse collagen fibers in the anterior human corneal stroma, *Investigative Ophthalmology & Visual Science*, Vol. 54, No. 12, 7293-7301, doi:10.1167/iovs.13-13150

[2] Sagara, T.; Hirano, S.; Uchida, T.; Suzuki, K.; Kumagai, N.; Nishida, T. (2005). Changes in central corneal thickness associated with topical corticosteroid administration in individuals with uveitis, *Investigative Ophthalmology & Visual Science*, Vol. 46, No. 13 (ARVO Annual Meeting Abstract), 4863

[3] Hatami-Marbini, H.; Etebu, E. (2013). An experimental and theoretical analysis of unconfined compression of corneal stroma, *Journal of Biomechanics*, Vol. 46, No. 10, 1752-1758, doi:10.1016/j.jbiomech.2013.03.013

[4] Kurpanik, R.; Gajek, M.; Gryń, K.; Jeleń, P.; Ścisłowska-Czarnecka, A.; Stodolak-Zych, E. (2024). Multiscale characterization of electrospun non-wovens for corneal regeneration: impact of microstructure on mechanical, optical and biological properties, *Journal of the Mechanical Behavior of Biomedical Materials*, Vol. 152, Paper 106437, 19 pages, doi:10.1016/j.jmbbm.2024.106437

[5] Pandolfi, A.; Manganiello, F. (2006). A model for the human cornea: constitutive formulation and numerical analysis, *Biomechanics and Modeling in Mechanobiology*, Vol. 5, No. 4, 237-246, doi:10.1007/s10237-005-0014-x

[6] Konomi, H.; Hayashi, T.; Nakayasu, K.; Arima, M. (1984). Localization of type V collagen and type IV collagen in human cornea, lung, and skin. Immunohistochemical evidence by anti-collagen antibodies characterized by immunoelectroblotting, *American Journal of Pathology*, Vol. 116, No. 3, 417-426
[7] Stanworth, A. (1953). Polarized light studies of the cornea: II. The effect of intra-ocular pressure, *The Journal of Experimental Biology*, Vol. 30, No. 2, 160-163, doi:10.1242/jeb.30.2.164
[8] Hahnel, C.; Somodi, S.; Weiss, D. G.; Guthoff, R. (2000). The keratocyte network of human cornea: a three-dimensional study using confocal laser scanning fluorescence microscopy, *Cornea*, Vol. 19, No. 2, 185-193, doi:10.1097/00003226-200003000-00012
[9] Komai, Y.; Ushiki, T. (1991). The three-dimensional organization of collagen fibrils in the human cornea and sclera, *Investigative Ophthalmology & Visual Science*, Vol. 32, No. 8, 2244-2258
[10] Liu, X. Y.; Wang, L. Z.; Ji, J.; Yao, W.; Wei, W.; Fan, J.; Joshi, S.; Li, D. Y.; Fan, Y. B. (2014). A mechanical model of the cornea considering the crimping morphology of collagen fibrils, *Investigative Ophthalmology & Visual Science*, Vol. 55, No. 4, 2739-2746, doi:10.1167/iovs.13-12633
[11] Meek, K. M.; Boote, C. (2004). The organization of collagen in the corneal stroma, *Experimental Eye Research*, Vol. 78, No. 3, 503-512, doi:10.1016/j.exer.2003.07.003
[12] Comninou, M.; Yannas, I. V. (1976). Dependence of stress-strain nonlinearity of connective tissues on the geometry of collagen fibres, *Journal of Biomechanics*, Vol. 9, No. 7, 427-433, doi:10.1016/0021-9290(76)90084-1
[13] Grytz, R.; Meschke, G. (2010). A computational remodeling approach to predict the physiological architecture of the collagen fibril network in corneo-scleral shells, *Biomechanics and Modeling in Mechanobiology*, Vol. 9, No. 2, 225-235, doi:10.1007/s10237-009-0173-2
[14] Jan, N.-J.; Lathrop, K.; Sigal, I. A. (2017). Collagen architecture of the posterior pole: high-resolution wide field of view visualization and analysis using polarized light microscopy, *Investigative Ophthalmology & Visual Science*, Vol. 58, No. 2, 735-744, doi:10.1167/iovs.16-20772
[15] Pinsky, P. M.; Datye, D. V. (1991). A microstructurally-based finite element model of the incised human cornea, *Journal of Biomechanics*, Vol. 24, No. 10, 907-922, doi:10.1016/0021-9290(91)90169-n
[16] Pandolfi, A.; Holzapfel, G. A. (2008). Three-dimensional modeling and computational analysis of the human cornea considering distributed collagen fibril orientations, *Journal of Biomechanical Engineering*, Vol. 130, No. 6, Paper 061006, 12 pages, doi:10.1115/1.2982251
[17] Whitford, C.; Studer, H.; Boote, C.; Meek, K. M.; Elsheikh, A. (2015). Biomechanical model of the human cornea: considering shear stiffness and regional variation of collagen anisotropy and density, *Journal of the Mechanical Behavior of Biomedical Materials*, Vol. 42, 76-87, doi:10.1016/j.jmbbm.2014.11.006
[18] Giraudet, C.; Diaz, J.; Le Tallec, P.; Allain, J.-M. (2022). Multiscale mechanical model based on patient-specific geometry: application to early keratoconus development, *Journal of the Mechanical Behavior of Biomedical Materials*, Vol. 129, Paper 105121, 13 pages, doi:10.1016/j.jmbbm.2022.105121
[19] Gomez, C.; Pinero, D. P.; Paredes, M.; Alio, J. L.; Cavas, F. (2024). Study of the influence of boundary conditions on corneal deformation based on the finite element method of a corneal biomechanics model, *Biomimetics*, Vol. 9, No. 2, Paper 73, 28 pages, doi:10.3390/biomimetics9020073
[20] Petsche, S. J.; Pinsky, P. M. (2013). The role of 3-D collagen organization in stromal elasticity: a model based on X-ray diffraction data and second harmonic-generated images, *Biomechanics and Modeling in Mechanobiology*, Vol. 12, No. 6, 1101-1113, doi:10.1007/s10237-012-0466-8
[21] Elsheikh, A.; Alhasso, D. (2009). Mechanical anisotropy of porcine cornea and correlation with stromal microstructure, *Experimental Eye Research*, Vol. 88, No. 6, 1084-1091, doi:10.1016/j.exer.2009.01.010
[22] Lopes, H.; Silva, S. P.; Machado, J. (2022). FEA approach for predicting the dynamic behaviour of cork-rubber composites, *International Journal of Simulation Modelling*, Vol. 21, No. 2, 237-248, doi:10.2507/IJSIMM21-2-599

[23] Hassell, J. R.; Birk, D. E. (2010). The molecular basis of corneal transparency, *Experimental Eye Research*, Vol. 91, No. 3, 326-335, doi:10.1016/j.exer.2010.06.021

[24] Akhtar, S.; Bron, A. J.; Salvi, S. M.; Hawksworth, N. R.; Tuft, S. J.; Meek, K. M. (2008). Ultrastructural analysis of collagen fibrils and proteoglycans in keratoconus, *Acta Ophthalmologica*, Vol. 86, No. 7, 764-772, doi:10.1111/j.1755-3768.2007.01142.x

[25] Simha, N. K.; Fedewa, M.; Leo, P. H.; Lewis, J. L.; Oegema, T. (1999). A composites theory predicts the dependence of stiffness of cartilage culture tissues on collagen volume fraction, *Journal of Biomechanics*, Vol. 32, No. 5, 503-509, doi:10.1016/s0021-9290(98)00185-7

[26] Jan, N.-J.; Brazile, B. L.; Hu, D.; Grube, G.; Wallace, J.; Gogola, A.; Sigal, I. A. (2018). Crimp around the globe; patterns of collagen crimp across the corneoscleral shell, *Experimental Eye Research*, Vol. 172, 159-170, doi:10.1016/j.exer.2018.04.003

[27] Xiang, Y.; Shen, M.; Xue, C.; Wu, D.; Wang, Y. (2018). Tensile biomechanical properties and constitutive parameters of human corneal stroma extracted by SMILE procedure, *Journal of the Mechanical Behavior of Biomedical Materials*, Vol. 85, 102-108, doi:10.1016/j.jmbbm.2018.05.042

[28] Daxer, A.; Misof, K.; Grabner, B.; Ettl, A.; Fratzl, P. (1998). Collagen fibrils in the human corneal stroma: structure and aging, *Investigative Ophthalmology & Visual Science*, Vol. 39, No. 3, 644-648

[29] Newton, R. H.; Meek, K. M. (1998). The integration of the corneal and limbal fibrils in the human eye, *Biophysical Journal*, Vol. 75, No. 5, 2508-2512, doi:10.1016/s0006-3495(98)77695-7

[30] Yu, J.-G.; Bao, F.-J.; Joda, A.; Fu, X.-A.; Zhou, S.; Wang, J.; Hu, X.-L.; Wang, Q.-M.; Elsheikh, A. (2014). Influence of glucocorticosteroids on the biomechanical properties of in-vivo rabbit cornea, *Journal of the Mechanical Behavior of Biomedical Materials*, Vol. 29, 350-359, doi:10.1016/j.jmbbm.2013.08.015

[31] Zeng, Y.; Yang, J.; Huang, K.; Lee, Z.; Lee, X. (2001). A comparison of biomechanical properties between human and porcine cornea, *Journal of Biomechanics*, Vol. 34, No. 4, 533-537, doi:10.1016/s0021-9290(00)00219-0

[32] Seiler, T. G.; Shao, P.; Frueh, B. E.; Yun, S.-H.; Seiler, T. (2018). The influence of hydration on different mechanical moduli of the cornea, *Graefe's Archive for Clinical and Experimental Ophthalmology*, Vol. 256, No. 9, 1653-1660, doi:10.1007/s00417-018-4069-7

[33] Boote, C.; Hayes, S.; Young, R. D.; Kamma-Lorger, C. S.; Hocking, P.; Elsheikh, A.; Inglehearn, C. F.; Ali, M.; Michael, K.; Meek, K. M. (2009). Ultrastructural changes in the retinopathy, globe enlarged (*rge*) chick cornea, *Journal of Structural Biology*, Vol. 166, No. 2, 195-204, doi:10.1016/j.jsb.2009.01.009

[34] Pitre, J. J.; Kirby, M. A.; Li, D. S.; Shen, T. T.; Wang, R. K.; O'Donnell, M.; Pelivanov, I. (2020). Nearly-incompressible transverse isotropy (NITI) of cornea elasticity: model and experiments with acoustic micro-tapping OCE, *Scientific Reports*, Vol. 10, No. 1, Paper 12983, 14 pages, doi:10.1038/s41598-020-69909-9

[35] Meek, K. M.; Tuft, S. J.; Huang, Y.; Gill, P. S.; Hayes, S.; Newton, R. H.; Bron, A. J. (2005). Changes in collagen orientation and distribution in keratoconus corneas, *Investigative Ophthalmology & Visual Science*, Vol. 46, No. 6, 1948-1956, doi:10.1167/iovs.04-1253